**Annales
Geophysicae**

Irregular HF radio propagation on a subauroral path during magnetospheric substorms

D. V. Blagoveshchensky[1]**, T. D. Borisova**[2]**, and J. W. MacDougall** [3]

[1]St. Petersburg State University of Aerospace Instrumentation, St. Petersburg, Russia
[2]Arctic and Antarctic Research Institute, St. Petersburg, Russia
[3]University of Western Ontario, London, Ontario, Canada

Abstract. The impact of the main ionospheric trough, sporadic structures, gradients and inhomogeneities of the subpolar ionosphere during substorms on the signal amplitude, azimuthal angles of arrival, and propagation modes for the radio path Ottawa (Canada)–St. Petersburg (Russia) was considered. This subauroral path with the length of about 6600 km has approximately an east-west orientation. The main goals are to carry out numerical modeling of radio propagation for the path and to compare the model calculations with experimental results. Wave absorption and effects of focusing and divergence of rays were taken into consideration in the radio wave modeling process. The following basic results were obtained: The signal amplitude increases by 20–30 dB 1–1.5 h before the substorm expansion phase onset. At the same time the signal azimuth deviates towards north of the great circle arc for the propagation path. Compared with quiet periods there are effects due to irregularities and gradients in the area of the polar edge of the main ionospheric trough on the passing signals. Propagation mechanisms also change during substorms. The growth of signal amplitude before the substorm can be physically explained by both a decrease of the F2-layer ionization and a growth of the F2-layer height that leads to a decrease of the signal field divergence and to a drop of the collision frequency. Ionospheric gradients are also important. This increase of signal level prior to a substorm could be used for forecasting of space weather disturbed conditions.

Keywords. Magnetospheric physics (Storms and substorms) – Ionosphere (Ionospheric disturbances) – Radio science (Radio wave propagation)

1 Introduction

It is well known that the main ionospheric trough (MIT), and the auroral oval, sporadic structures, and belt of ionospheric inhomogeneities concentrated southward the oval impact on HF radio propagation on the paths located in the area of invariant latitudes 50–75° (Blagoveshchensky, 1981; Blagoveshchensky et al., 1982; Hunsucker and Hargreaves, 2003; Milan et al., 1997; Siddle et al., 2004a; Siddle et al., 2004b). Lateral signal reflections, backscatter, quick fading of signals at a receiving point, and unusual modes of propagation are observed. However, geomagnetic disturbances occurring in the auroral and subauroral ionosphere of the Earth, lead to even more complicated (anomalous) conditions of HF radio propagation in the subpolar regions (Blagoveshchensky and Zherebtsov, 1987; Blagoveshchensky and Borisova, 2000; Blagoveshchensky et al., 1996, 2005b; Milan et al., 1998, 1996). This happened because there are additional small- and large-scale irregularities of the ionosphere during magnetospheric storms and substorms, (Blagoveshchensky et al., 2003a, 2003b; Buonsanto, 1999; Gonzalez et al., 1994; Lastovicka, 2002; Lyons, 1996). Also all parameters of the ionosphere and the large-scale structures in the subauroral region (MIT, gradients, sporadic ionization and so on) show more change in their morphology when the substorm/storm intensity is greater. Earlier, experimental investigations of the HF radio propagation on high-latitude paths were carried out by many authors (Blagoveshchensky, 1981; Hunsucker and Hargreaves, 2003; Angling et al., 1998; Milan et al., 1998, 1996; Warrington and Stocker, 2003). These studies revealed the main peculiarities of HF radio propagation on the subauroral and auroral paths. However, special measurements of signal amplitude and azimuths of arrival angles at the receiving point of paths and information about basic propagation modes during substorms are not enough to understand how this region affects radio propagation. A
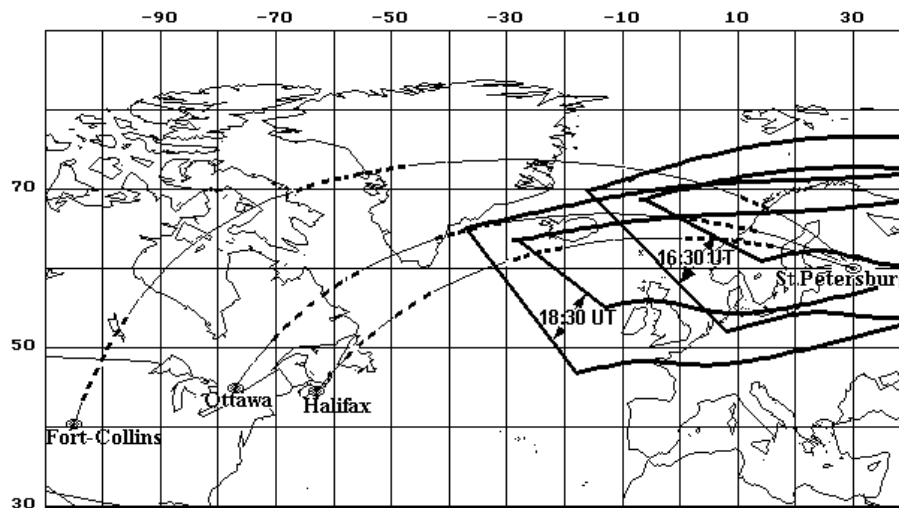
Fig. 1. Great circle radio paths from Canada to St. Petersburg. Dashed parts of the radio paths show where ionospheric reflections would occur. The locations of the main ionospheric trough from a model by Halcrow and Nisbet (1977) at 16:50 and 18:40 UT are shown for 6 January 1982 and K_p=2. The trough contours show the outer boundaries and the inner boundaries of the trough walls.

more detailed analysis of the propagation is necessary. This is important for questions of radio communication organization, over horizon location, direction finding, navigation and so on at high latitudes (Blagoveshchensky and Zherebtsov, 1987; Goodman, 1992).

In this paper, the impact of some geophysical phenomena mentioned above during magnetospheric substorms on the level of electromagnetic field and azimuthal deviation of radio signal at the receiving point as well as mechanisms (modes) of propagation for the subauroral radio path Ottawa–St. Petersburg (D=6600 km) is analyzed. This transatlantic path, Fig. 1, connecting Canada with Russia, was investigated as part of an international collaboration.

There are three goals to this study: (i) to study in detail the behavior of both the levels of signal amplitude and the azimuthal angles of arrival from experimental measurements, (ii) to carry out numerical modeling of radio propagation and compare model calculations with experimental results for better understanding of the physical mechanisms involved when the signal passes through the HF radio channels, (iii) to make quantitative estimates of ionospheric parameters influences on the value of the electromagnetic field of the HF radio signal.

Before solving these tasks, it must be emphasized that some applicable results were obtained by the authors in earlier studies. To begin with there are effects of signal amplitude growth and azimuth variations during substorms on different radio paths. Relevant investigations were presented in (Blagoveshchensky and Borisova, 2000; Blagoveshchensky et al., 2005, 1996). It has been found experimentally that the effect of amplitude growth and azimuth variations take place on both short (one-hop) and long (multi-hop) high-latitude paths. Figure 1 shows the Fort Collins–St. Peters-

burg, and Halifax–St. Petersburg paths in addition to the Ottawa–St. Petersburg path. These two additional paths are also subauroral and they are located along the main ionospheric trough (MIT) (see trough locations shown in Fig. 1). Let us describe an example of signal amplitude variations at the receiving point during a substorm on 28 December 1978 for the Fort Collins–St. Petersburg path (D=7200 km, f=15 MHz). The moment of substorm expansion phase onset is designated by T_o. There is signal amplitude growth within ∼1 h before T_o, further a drop of amplitude during the substorm expansion phase, and then an amplitude growth near the end of the substorm. Similar signal amplitude variations occur on the Halifax–St. Petersburg path (D=7200 km, f=15 MHz) for a substorm on 6 January 1982.

At present, a full physical explanation of the signal amplitude growth does not exist, however, there is a good reason to believe that this effect is associated with so called "the main ionospheric effect during substorm". In the paper Blagoveshchensky et al., 2005a, the "main effect" was studied for an averaging of data from a group of subauroral and midlatitude European ionospheric stations (Blagoveshchensky et al., 1996, 2003a). There is a definite regular variation of both the F2-layer's critical frequency and height of ionization maximum of F2 during substorms. The substorms used had a sharp onset at time T_o (Blagoveshchensky et al., 2003a). The study shows deviations in percent relatively to the quiet level of ionospheric parameters for the growth (6 h before T_o), expansion (T_o) to (T_o+3) and recovery (T_o+3) to (T_o+6) phases of a substorm. 2–6 h before the substorm expansion phase development there is a sharp growth of the F2-layer ionization ($\Delta foF2$=+ 25%). Then the ionization decreases smoothly up T_o ($\Delta foF2$=–30%). After T_o, during the expansion phase lasting about three hours, both slight

growth and then decrease of ionization take place. During the substorm recovery phase, (T_o+3) to (T_o+6), there is more intensive growth (ΔfoF2=+30%) and then decrease of ionization. The height of the F2-layer maximum has a tendency to increase smoothly 2 h before the T_o moment up to ΔhmF2=+30%. After the expansion phase onset, during the next three hours, there is a little decrease and then growth of the F2-layer maximum height to the end of the expansion phase and then a further smooth decrease to the quiet level. Variations of the sporadic E layer critical frequency, ΔfoE$_s$, show some oscillations with a little growth ($\sim$15%) starting 3 h before T_o and then with growth (+30%) within the expansion phase. Note that these E$_s$ variations are from a subset of the whole group of ionosonde measurements – the E$_s$ effects are seen mainly on ionosondes located near the auroral oval.

Thus, in the previous papers the following was discovered: There is an amplitude growth of propagating signals before substorms on HF radio paths, and associated with the substorms ionospheric changes called the "main ionospheric effect". These effects were found experimentally by means of oblique ionospheric sounding and vertical ionospheric sounding using a network of stations (Blagoveshchensky et al., 1996; Blagoveshchensky et al., 2005a). In this paper we are trying to connect the ionospheric changes with the changes in propagation signal strength for a better understanding of the physical phenomena that are involved.

2 Experiment on the Ottawa–St. Petersburg path

Empirical measurements of electromagnetic field level and azimuthal angles of arrival of radio signal with a frequency f=14 670 kHz from an Ottawa transmitter (44° N; 77° W) were carried out in 1982 at a receiving point located nearly St. Petersburg (59.5° N; 30° E).

Why was the Ottawa–St. Petersburg path chosen for this studying? Firstly, our interest is with the northern sector of the Atlantic from Russia to Canada because ionospheric parameters variations during substorms have been studied in this sector (for example Blagoveshchensky et al., 2005a). Secondly, the radio path Ottawa-St. Petersburg (D=6600 km) is a subauroral one directed approximately east-west (see Fig. 1). The MIT, and auroral and subauroral ionospheric irregularities along with temporal and spatial variations of ionospheric ionization and gradients impact on the character of HF radio wave propagation on this path. In the present paper, experimental data for the winter season of 1982 during evening and premidnight hours from 18 to 23 MDT (MDT=UT + 3) was considered.

Our radio direction finding system in St. Petersburg had a revolving antenna. The choice of two directions was executed by relevant program. The first one, (308±5)°, is intended to receive the CW signals passing along the great circle arc from Ottawa to St. Petersburg. The second one, (340±20)°, is intended to receive the same signals going

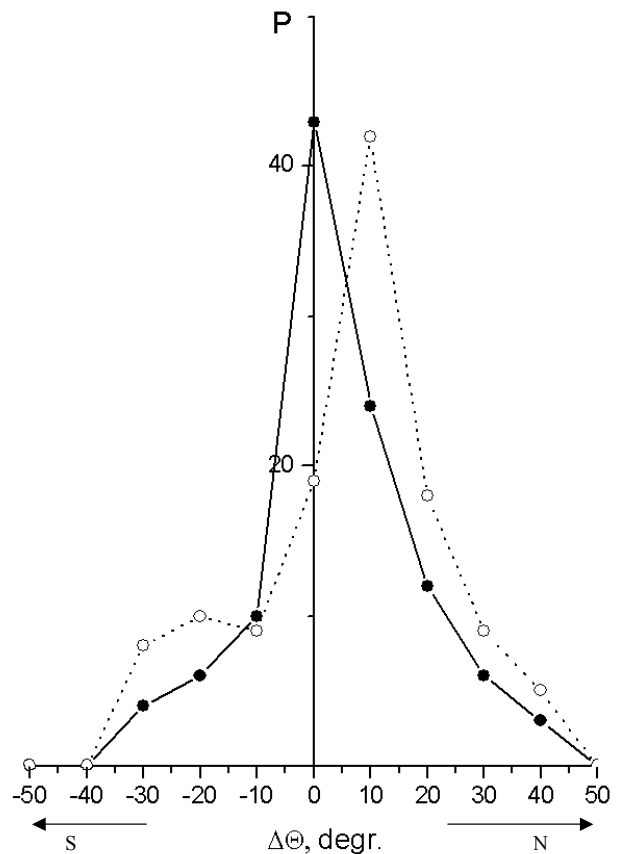**Fig. 2.** Probabilities P(%) of the azimuthal deviations $\Delta\Theta$ for the Ottawa-St. Petersburg path (f=14670 kHz) for two levels of magnetic activity $\Sigma K_p < 16$ (solid line) and $16 < \Sigma K_p < 25$ (dotter line) for the measurements carried out during the winter season of 1982.

from the north directions due to scattering predominantly. These channels were working independently. The scattered signals have being received after the main signal with a delay about one second. The accuracy of receiving is ±2°.

Azimuthal variations $\Delta\Theta$ were determined as deviations from the great circle path direction. Figure 2 shows an example of the probabilities P of azimuthal deviations for the path Ottawa–St. Petersburg (f=14 670 kHz) for two levels of magnetic activity $\Sigma K_p < 16$ and $16 < \Sigma K_p < 25$. The probability P of the azimuthal deviations are a distribution of measurements made by a receiver/antenna with directional capability. Curves on figure were determined for all period of observations, about 2000 measurements. One can see from Fig. 2 that under weakly disturbed conditions ($\Sigma K_p < 16$, solid line) the lateral deviations on the path are nearly symmetrical relatively zero, the great circle direction. However, under moderate disturbed conditions ($16 < \Sigma K_p < 25$, dotted line) the lateral deviations from the north, at +10 deg, are sharply increased. Obviously, they are caused by the appearance of gradients and intensive irregularities on the polar edge of the MIT during disturbances.
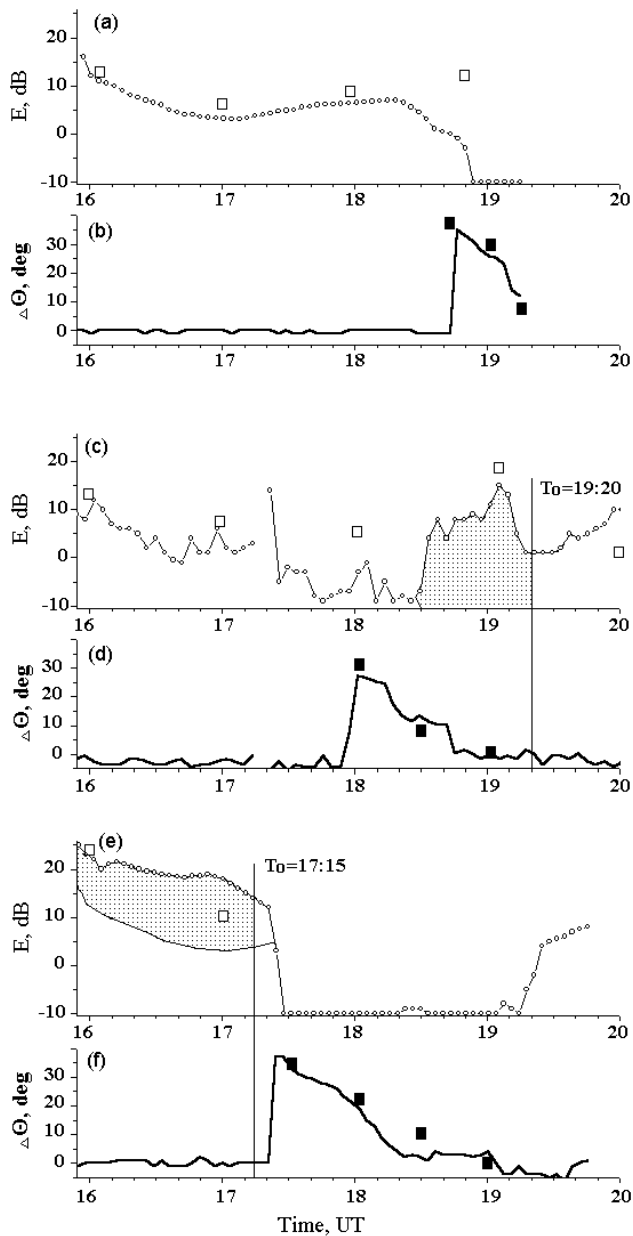
Fig. 3. Variations of the signal strength E and azimuthal deviations of arrival angles $\Delta\Theta$ at the receiving point of the Ottawa–St. Petersburg path during the quiet day of 14 January 1982 **(a)** and **(b)**, the day of 6 January with a moderate substorm **(c)** and **(d)** and the day of 8 January with an intense substorm **(e)** and **(f)**. T_o is the substorm expansion phase onset, the operational frequency is f=14 670 kHz, squares are numerical modelled values.

Figure 3 demonstrates some results of measurements of electromagnetic field strength (E, dB relatively 1 microV/m) and angular deviations ($\Delta\Theta$, degrees) on the Ottawa–St. Petersburg path. Three days were chosen for analysis. These days selected are the most typical and representative and they have substorms with sharp onsets (the T_o moment). Sub-

storms are characterized by different intensities and mean values of K_p- indexes: 14 January 1982 is a quiet day, K_p=1– (Figs. 3a and 3b); 6 January 1982 is a day with a moderate substorm, K_p=2o (Figs. 3c and 3d); 8 January 1982 is a day with an intense substorm, K_p=3- (Figs. 3e and 3f). The substorms starts, T_o moments, are identified from the AE indexes for 6 January 1982 and 8 January 1982.

From Figs. 3a and 3b one can see that the time of a sharp drop of the signal strength E on the radio path under quiet conditions (18:40 UT) is associated with a transition from reflection of radio waves to their scatter from ionospheric irregularities located on the polar edge of the trough (PET). The irregularity scattered signal is very small but measurable even as the signal appears have hit a "zero" value. A great increase of $\Delta\Theta$ values takes place at the moments of a sharp decrease of the signal strength and the $\Delta\Theta$ values themselves are mainly positive ones. Therefore, there the scattered signals come from the north directions. According to Fig. 3b, $\Delta\Theta$ deviations on the path have a clear tendency to decrease with time. This smooth drop is explained by the PET moving southward during premidnight hours.

An analysis of data presented in Figs. 3c and 3e shows that the signal strength level on the Ottawa–St. Petersburg path before the moment T_o as compared with a quiet day is increased by 15 dB. This can be seen on 6 January 1982 (Fig. 3c) where an increase of signal strength takes place from 18:30 to 19:20 UT and the substorm expansion phase onset is T_o=19:20 UT. For 8 January 1982 (Fig. 3e) a growth of signal level (relative to the quiet day curve shown below the shaded region on the figure) takes place from 16:00 to 17:15 UT and T_o=17:15 UT. Therefore before the T_o moment one can see the effect of signal level growth which as a rule exists during about one hour (the shaded areas on Figs. 3c and 3e). For more intensive substorms, as can be seen from Figs. 3d and 3f, the moment of both the transition from reflection to scatter and the increase of $\Delta\Theta$ occurs during earlier hours because the PET is additionally moved southward during disturbances. For the Ottawa–St.Petersburg path these moments are: 18:40 UT (Fig. 3b), 18:00 UT (Fig. 3d) and 17:20 UT (Fig. 3f). Thus, the substorm effect in $\Delta\Theta$ values at the beginning of substorm development is manifested at earlier time as compared with the quiet period and this effect is associated with the beginning of the impact of auroral ionosphere irregularities which are concentrated northward of the great circle arc. For the Ottawa–St.Petrsburg path those are the irregularities located on the PET.

3 Modeling the radio propagation

Ray tracing calculations of propagation parameters on the Ottawa–St. Petersburg path for comparison with experimental data were carried out. Model calculations using the "model of HF radio channel" (Borisova et al., 1986) were performed using the approximation of 2-D geometrical

optics taking into consideration the smooth horizontal irregularities of the ionosphere.

3.1 Model approach for signal strength E calculation

For description of spatial and temporal variations of the propagation medium the "global ionospheric model" (the IZMIRAN ionospheric model which is similar to the international reference ionosphere model) is used in "the model of HF radio channel". The global model is constructed by unification of known models of separate ionospheric E, F1, and F2 layers and the interlayer valleys (Chernyshev and Vasil'eva, 1975; Anufrieva and Shapiro, 1976; Rawer et al., 1976). Ionospheric electron concentration variations due to substorm impact were described by using a special program block which allows for ionospheric correction. The regularities of ionospheric behavior during a substorm, the "main effect", were used for this.

Input parameters for the model are: the geographical coordinates of the transmitter and receiver, the radiation patterns of receiving and transmitting antennas, the date and time, the operational frequency f of the radio signal, and a measure of the prevailing geophysical conditions using Wolf number and magnetic activity level with given K_p–index (Blagoveshchensky and Borisova, 1989). The model of the HF radio channel permits calculation of some characteristics of radio propagation on a given path: the ray trajectories, the group and phase paths, the mode types, the Doppler frequency variations, arrival angles in the vertical and horizontal planes, and the electromagnetic field strength E.

For calculation of the field strength E at a receiving point, the following expression from (Ginzburg, 1967; Al'pert, 1972) was used

$$E = \frac{173.2\sqrt{P}}{R_E \sin D_\Theta} \sqrt{\frac{\sin \alpha_{tr}}{R_E \cos \alpha_{rec} \left| \frac{\partial D_\Theta}{\partial \alpha} \right|}} \cdot \exp(-\Gamma) \cdot \prod_{i=1}^{N} \rho_i \quad , (1)$$

where P is a source power, R_E is the Earth's radius; D_Θ is the angle length of the path along the Earth's surface; α_{tr} and α_{rec} are the elevation angles of transmitter and receiver; $\partial D_\Theta/\partial \alpha$ is a coefficient of space divergence of rays; ρ is a coefficient of losses due to reflection from the Earth's surface which depends on signal frequency and surface characteristics; N is a reflections number; Γ is a coefficient of losses due to signal propagation in the ionosphere.

For the HF range, the expression for the loss coefficient Γ can be presented using the group L_{gr} and phase L_{ph} paths

$$\Gamma = 1/(2c)v(r)[1/n(r) - n(r)]dr = \Sigma v_i \cdot (L_{gr} - L_{ph}), (2)$$

where $r = h + R_E$, h is a height from the Earth's surface and R_E is the Earth's radius; $n = \varepsilon^{1/2}$ is a refraction coefficient under condition that an impact of collision on the dielectric permeability is neglected; c is the speed of light; v_i is the effective collision frequency of electrons and a value of v_i is
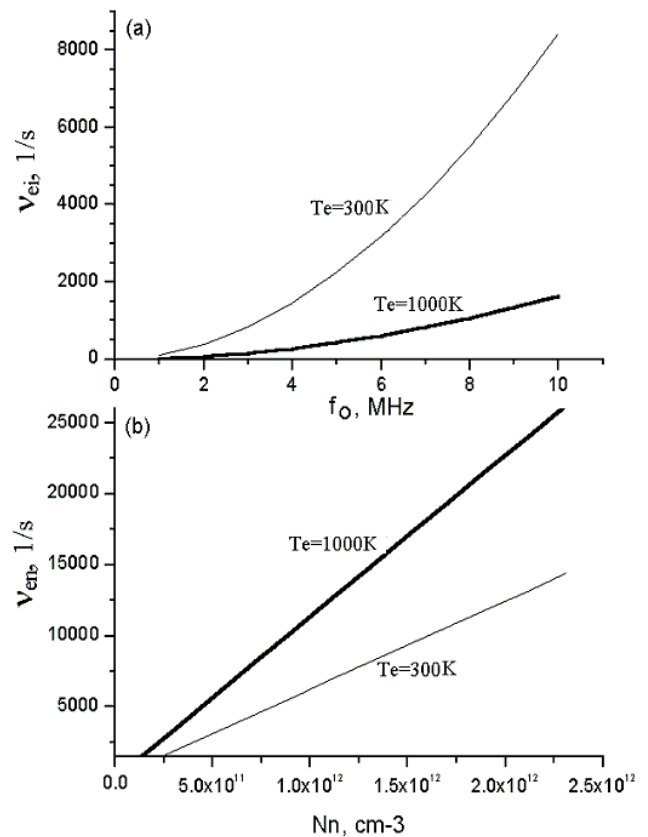

Fig. 4. Relationships between the collision frequency v_{ei} and the critical frequency fo **(a)** and between the collision frequency v_{en} and the concentration of neutrals **(b)** for two levels of electron temperature Te=300 and 1000 K.

constant on the i-step of summarizing (after transition from integration to summarizing).

At first, the coefficient Γ was determined by Eq. (2) through integration along the radio path and then calculation of the electromagnetic field strength E at the receiving point by Eq. (1) was done.

3.2 Calculation of the electron collision frequency in the ionosphere

The value of effective electron collision number v_{eff} is a sum of collision frequencies

$$v_{eff} = v_{ei} + v_{en} + v_e, \tag{3}$$

where v_{ei} is a frequency of collisions electrons with ions; v_{en} is the same but with neutrals; v_e – with electrons. For the ionospheric plasma, v_e value can be neglected in Eq. (3) because it is less than v_{ei} and v_{en} by two orders of magnitude.

There are two expression by (Ginzburg, 1967) and (Nicolet, 1953) to determine v_{ei} and v_{en} parameters

$$v_{en} = (3.6 - 5.4) \cdot 10^{-10} N_n T_e^{1/2}$$

$$v_{ei} = 12.65 \cdot N_e \cdot \lg(220 \cdot T_e/N_e^{1/3})/T_e^{3/2}, \tag{4}$$

where N_n is the concentration of neutral particles (particles.cm^{-3}); N_e is the electron (ion) concentration (electrons.cm^{-3}); T_e is the electron temperature (K); lg is the decimal logarithm.

From Eqs. (4) one can see that collision frequencies ν_{ei} and ν_{en} depend on both the concentrations and the electron temperature. Variations of the regular electron temperature for the ionospheric F-layer in middle latitudes are limited to the range 300–1500° (Al'pert, 1972).

Figure 4 shows calculations of the collision frequencies ν_{ei} and ν_{en}. Figure 4a shows ν_{ei} versus the critical ionospheric frequency fo=$8.98 \cdot 10^3 \cdot Ne^{1/2}$, and Fig. 4b shows ν_{en} versus the concentration of neutrals, N_n. One can see from Fig. 4a that some decrease of electron concentration, which occurs during the period before a substorm onset, leads to a drop of the collision frequencies ν_{ei}.

An analysis of numerical calculations of the effective collision frequencies ν_{eff} using Eqs. (3) and (4) allows us to estimate quantitatively the impact of parameters N_e, N_n, and T_e on the ν_{eff} values for the ionospheric E- and F2-layers. In later calculations of ν_{eff} for determination of the signal strength E, the influence on ν_{en} of the height of ionospheric E-layer was important because for the F2 layer $\nu_{ei} \gg \nu_{en}$. Our calculations were carried out using the MSIS model (http://nssdc.gsfc.nasa.gov/space/model/models/msis.html) which show that the concentration of neutrals is decreases sharply with a height h. For the ionospheric E-layer $N_n \sim 1 \cdot 10^{+12}$, and for the F2-layer $N_n \sim 1 \cdot 10^{+9}$, therefore the ν_{en} value is decreased by three orders of magnitude, see Fig. 4b.

It is of interest to consider the effects of ν_{eff} variations during the substorm growth phase for which the ionospheric parameters vary according to the "main effect" regularities mentioned in the introduction. Namely, during the time period 1–2 h before the substorm onset, when increases of the signal strength E is observed by up to 20–30 dB, the critical frequencies foE$_s$ and foF2 drop by 20 and 30%, respectively and the height of the F2-layer maximum increases by 30%. Due to ionospheric changes associated with a height change, we can easily estimate the local changes in ν_{eff} using Eqs. (3) and (4):

1. In the ionospheric F2-layer, if there is a temperature growth by 200–400 K associated with the height change, and a simultaneous decrease of critical frequencies by 30–40% this leads to a drop of ν_{eff} values by a factor of four.

2. The appearance of an E$_s$ sporadic layer on the path causes some changes of the collision frequency value too. A decrease of critical frequency at the heights of E-layer by 10–20% leads to a drop of ν_{eff} value in the E region of $\sim$20%.

What are the possible causes and consequences of increasing the F2-layer height 1–2 h before the substorm onset? It is known (Buonsanto, 1999) that under magnetically disturbed conditions within the middle latitude ionosphere a growth of the F2-layer maximum height is observed. One of the causes of this growth can be an electric field with west-to-east direction. The middle latitude ionosphere during substorms is per-

turbed by both electric fields and internal atmospheric gravity waves (AGWs). The effect of AGW is similar to an electric field effect. According to (Rishbeth and Garriott, 1969; Buonsanto, 1999) vertical height change of the F-layer due to AGWs influence can be about 100 km which is more than an electric field impact. As is well known, the magnetospheric electric field, directed from dawn-to-dusk, is increased some minutes after a turning of the vertical component of the IMF B_z to southward. Almost simultaneously, the dawn-to-dusk electric field in the polar region and corresponding fields in the middle latitudes are increased. Electric currents and magnetic disturbances of the DP$_2$ type also appear. There is also the development of polar electrojets and other phenomena corresponding to the substorm growth phase which will happened 0.5–1 h later. Therefore, an interval from the B_z turning southward to the onset of electrojets development exists when the existence of the AGW generated during substorms is unlikely and a growth of the F2-layer maximum height can be explained by just the influence of electric fields.

Thus, estimations show that the specific decreases of electron concentration in the E- and F-layers before a substorm contribute to a drop of the effective collision frequency ν_{eff} and therefore to an increase of signal strength E. It is not immediately obvious whether this would give a large or small change in radio signal strength. Numerical modeling was carried out to find how great is the growth of signal strength E at the receiving point of the radio path before a substorm.

3.3   Calculations of the signal strength values

Some different calculations of electromagnetic field strength E on the Ottawa–St. Petersburg path using different values of the ionospheric E- and F2-layer parameters were carried out. The critical frequency foF2, the height of F2-layer maximum hmF2, and the critical frequency foE$_s$ were varied under the assumption that the ionosphere is homogeneous along the radio path. Calculations were carried out for the radio signal frequency f=14670 kHz.

• Model results #1: In Fig. 5 are shown the calculated results of the signal strength, E, received for the propagation mode 2F2 (2 hop F2 mode) that is typical for the frequency f=14670 kHz on the Ottawa–St. Petersburg path. Figure 5a demonstrates the association of signal strength E with the critical frequency foF2. A relationship between E and hmF2 is shown in Fig. 5b. Figure 5c illustrates the E variations as a function of both the hmF2 increasing and the foF2 decreasing simultaneously. One can see from Figs. 5a, 5b, and 5c that the signal strength E depends on the range of the ionospheric parameters variations.

– It is seen from Fig. 5a that a decrease of the foF2 value by 30–50% leads to a growth of E value of only 1–2 dB if the critical frequency foF2 is about 7 MHz.

– Figure 5b shows that an increase of the hmF2 value by 30% causes a growth of E value by ∼3 dB when hmF2<320 km.

– Calculations results presented in Fig. 5c show that both a growth of hmF2 from 290 to 315 km and a decrease of foF2 from 9.0 to 6.5 MHz simultaneously will lead to the growth of radio signal level by ∼10 dB.

Further model calculations gave the following results:

– Increasing the temperature from 300 to 1000 K in the F2-layer causes an increase of E value by 1–3 dB.

– A drop of the critical frequency foE$_s$ by 15% leads to a growth of E value by 6–10 dB.

• Model results #2: The natural distribution of ionospheric plasma along the radio path is characterized as a rule by an existence of gradients of the critical frequency foF2 and the F2-layer height hmF2. Modeling the propagation parameters, taking into consideration the ionospheric gradients of the F2-layer ∂foF2$/\partial$D and ∂hmF2$/\partial$D, has showed that these gradients can very significantly change the ray trajectory in the ionospheric channel. As a consequence, the spatial divergence of rays $\partial\theta/\partial\alpha$ is being changed too. An increase of signal strength E can reach ∼10 dB for both ∂foF2$/\partial$D=–(0.2–0.5) MHz / 1000 km and ∂hmF2$/\partial$D=(2–5) km / 1000 km values that are typical for the evening hours on the Ottawa–St. Petersburg path. Therefore due to the existence of sharper ionospheric gradients, $\partial\theta/\partial\alpha$ value can increase the signal strength E by 10–15 dB. The calculations yield the results that ionospheric parameter variations, similar to those that really happen in the F2-layer, lead to significant propagation trajectory variations. In the case of a drop of ionospheric ionization maximum (the evening hours on the path), the operational frequency approaches to the maximum observed frequency (MOF) and signal strength is increased due to a focusing effect (or a divergence decrease).

Therefore the main results of modeling are the following: A growth of the signal strength E before the T_o moment of a substorm can be explained by the joint impact of several effects: a decrease of the F2-layer ionization along the radio path (1–2) dB, a growth of the F2-layer height (∼3) dB, an existence of regular ionospheric gradients (10–15) dB, and a drop of the effective collision frequency ν_{eff}–(1–3) dB. Their joint action can lead to a rise of the signal strength E before the substorm onset by 20–30 dB which is observed experimentally.
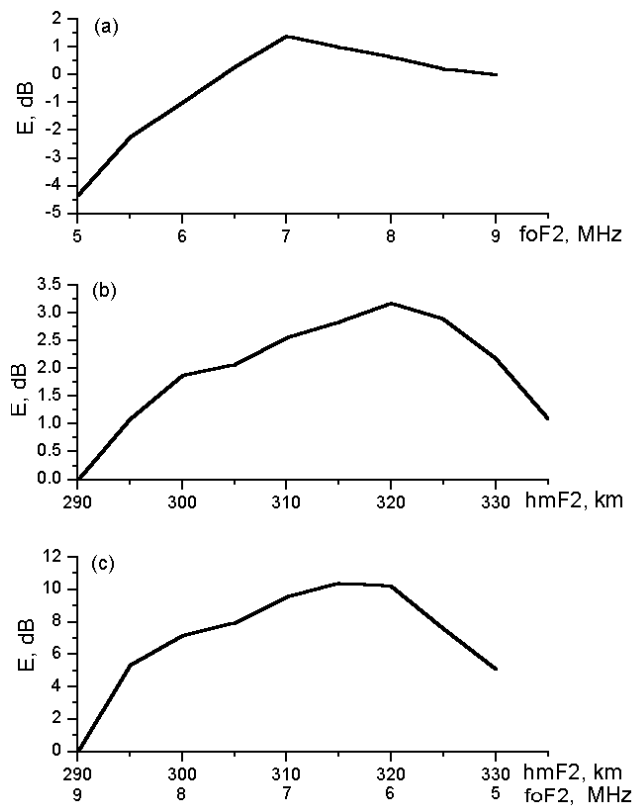

Fig. 5. Calculation results of the signal strength E at the receiving point of the Ottawa–St. Petersburg path for the frequency f=14 670 kHz versus foF2 **(a)**, hmF2 **(b)**, and foF2 and hmF2 simultaneously **(c)**.

4 Comparison of modeling results with experimental data

4.1 Variations of signal strength and propagation mechanisms during the substorm period

Ray tracing calculations on the Ottawa–St. Petersburg path have shown that the propagation modes 2F2 and 3F2 are possible under quiet geomagnetic conditions. Figure 6 shows some modeled ray trajectories. The mode 4F2 is negligible because of its small signal strength as compared with modes 2F2 and 3F2. In Fig. 6b the radio waves are skimming the limb of the Earth (note that there are no ground reflections). The signal receiving in St. Petersburg is possible due to scatter by the field-aligned ionospheric inhomogeneities located in the area of polar edge of trough at both the E- and F- layers levels. The second reflection of mode 3F2 happens in the area of auroral oval.

Variations of parameters ΔfoF2, ΔhmF2, and ΔfoE$_s$ of the subauroral and partly auroral ionosphere during three phases of substorm, the "main effect", were taken into consideration for ray tracing calculations along the path. Shown in Fig. 3c (square symbols) are the signal strength E values for
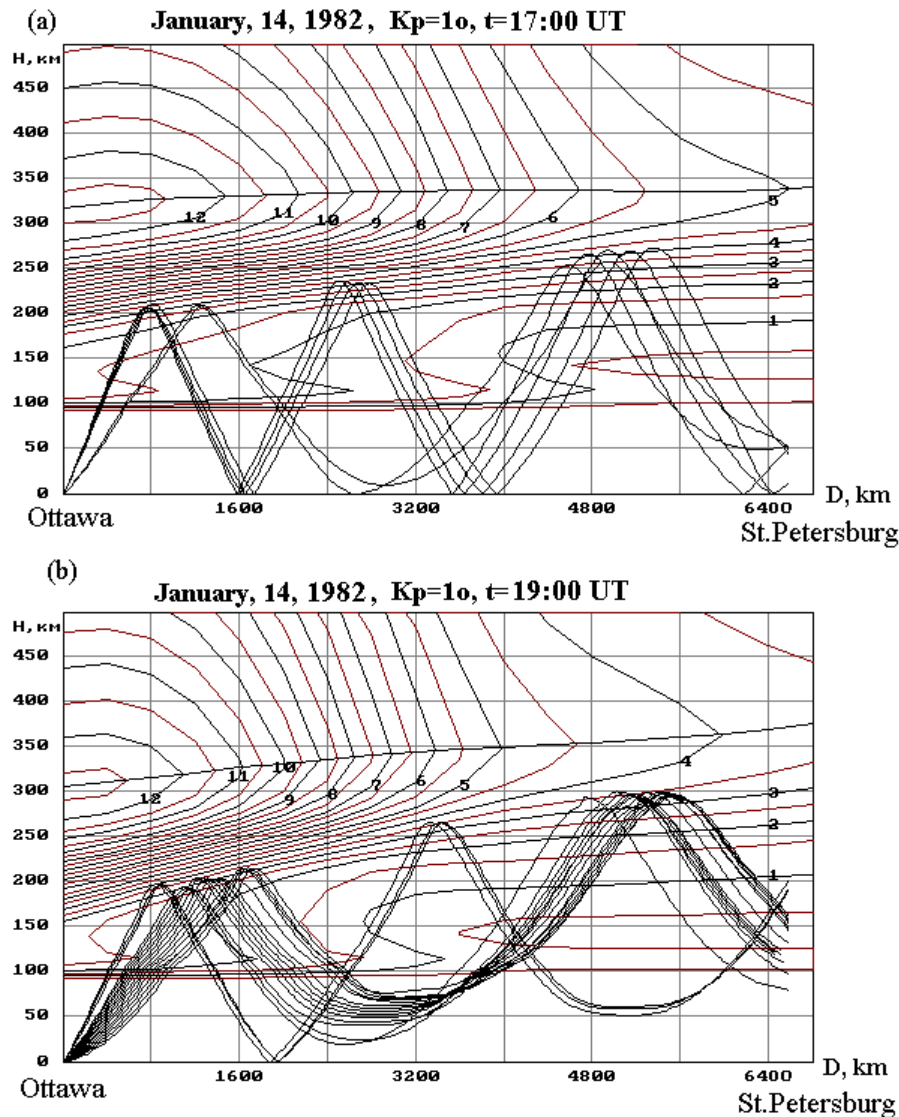
Fig. 6. Ray tracing calculations for the Ottawa–St. Petersburg path: the multi-hop propagation mechanism at 17:00 UT **(a)**, and the wave capture into the ionosphere by the regular longitudinal gradients of the ionosphere at 19:00 UT **(b)**. Values of the critical frequency fo on the figure contours are in MHz.

6 January 1982. Here the substorm expansion phase onset is T_o=19:20 UT. Modeling results yield that during the growth phase from 18:20 to 19:20 UT the modes 2F2 and 3F2 are possible whereas under the quiet conditions (without substorms) and for the same time from 18:20 to 19:20 UT the model calculations give the result that no propagation is possible for the path. Referring to Fig. 3c, we show good agreement from our modeling for both the intense signal before the substorm expansion phase and the overall pattern of signal variations during the entire substorm interval. During the growth phase, 18:20–19:20, the E value is significantly greater than under quiet conditions for this time interval (see shaded region on Fig. 3c).

An analysis of ray tracing calculations showed that the main mechanism of propagation for the path during day-time is multi-hop by F2 reflections. For the evening hours, there is a wave capture into the ionosphere by the regular longitudinal gradients. In the case when the terminator crosses the path, the signal receiving after 17:00 UT is possible only due to wave removal from the ionosphere on the night side. The removal mechanism itself is caused by inhomogeneities located in the areas of the terminator, MIT, and auroral oval. There is either refraction by the horizontal gradients of electron concentration near the polar edge of trough or field-aligned scatter by auroral irregularities in the ionospheric E- and F-layers. For modeling we assumed some F2-parameters

in the area of assumed field-align scatter in order to model the azimuthal deviations during the period from 16:00 to 20:00 UT. We used $hmF2$=300–340 km, $foF2$ =4.0–3.5 MHz. Figures 3b, 3d, 3f demonstrate some model calculations of azimuthal deviations $\Delta\Theta$ simultaneously with experimental data on the Ottawa–St. Petersburg path for 14, 6, and 8 January 1982. The calculation values are shown by squares. One can see acceptable agreement between the measured and the calculated data.

4.2 Interpretation of experimental and modeling data

4.2.1 The quiet day of 14 January 1982

a) The signal strength E variations

An empirical pattern E(t) is presented in Fig. 3a. It is of interest to consider the relevant modeling results. According to the propagation model, the modes 2F2, 3F2, and 4F2 are observed up to 17:00 UT on the path that is seen from Fig. 6a for t=17:00 UT. After 17:00 UT the mode 2F2 is absent at the receiving point because it is skimming the limb of the Earth (see Fig. 6b). At this time the regular propagation 2F2 mechanism is no longer operational. The mode 3F2 is also skimming and the signal amplitude must decrease according to the model. However, one can see from Fig. 3a that the signal strength from 17:30 to 19:00 UT is quite intensive. This can be explained by the impact of the terminator or the butt-end sunset wall of the MIT on the reflection point nearest to the receiver of the path from 17:00 to 19:00 UT. This leads, according to calculations, to an appearance of the modes 2F2 and 3F2 as a result of their bending. After 19:00 UT the impact of the terminator is over according to the model, the modes 2F2 disappear, and the signal strength is sharply decreased. Namely, the regular propagation along the great circle arc is finished and a scatter from the PET arises, Fig. 3a.

b) The azimuthal variations $\Delta\Theta$, Fig. 3b

According to model calculations, around 19:00 UT it is possible to receive the signals scattered by the magnetic field-align irregularities of the ionospheric F-layer located in the PET area. Similar conclusion is confirmed by experimental data in Fig. 3b where the sharp jump of $\Delta\Theta$ value followed by decreasing $\Delta\Theta$ takes place.

4.2.2 The day of 6 January 1982 with a moderate substorm.

a) The signal strength E variations is shown in Fig. 6c

According to model calculations, wave propagation on the path up to 17:00 UT is realized by modes 2F2, 3F2, and 4F2. After 17:00 UT there is only mode 3F2. Calculations

results (square symbols) and experimental data in Fig. 3c can be considered as comparable. According to experiment from 18:30 to 19:20 UT, a significant increase of signal strength takes place. This increase of signal strength, as was mentioned above, is associated with the substorm expansion phase onset at T_o=19:20 UT. Modeling results of the effect of signal strength growth before the T_o moment is confirmed by experimental data.

b) The azimuthal variations $\Delta\Theta^o$, Fig. 3d

According to calculations, the conditions of receiving the signals, scattered from the PET, arise after 18:00 UT. At the same time, a sharp jump of $\Delta\Theta^o$ values takes place according to the experimental data shown in Fig. 3d.

4.2.3 The day of 8 January 1982 with an intense substorm

1. The signal strength E variations, Fig. 3e

Here the model calculations show that the regular mechanism of radio wave propagation is similar to the mechanism of the quiet day, 14 January and the regular multi-hop wave propagation is finished at 17:30 UT. The received signal disappears after 17:30 UT as shown by experimental data in Fig. 3e. Some growth of signal strength after 19:30 UT in Fig. 3e is caused by rays propagating by unusual paths due to refraction bending at the PET.

2. The azimuthal variations $\Delta\Theta^o$

One can see from Fig. 3f that at 17:20 UT there is a sharp deviation of $\Delta\Theta^o$ values. According to modeling data, after this time radio signals scattered by field-aligned irregularities at the PET can be received.

5 Conclusions

1. Some peculiarities of HF radio wave propagation on the path Ottawa–St. Petersburg during magnetospheric substorms were revealed using experimental data and numerical modeling. Model calculations are in a good agreement with the experimental results confirming that the model used suitable physical mechanisms of propagation and suitable choice of parameters for the radio channels.

2. During substorms, growth of the signal amplitude is observed 1–1.5 h before the substorm expansion phase onset. At the same time, there may be azimuthal deviations of the received signal, compared to the great circle path, due to the effects of ionospheric irregularities and gradients in the area of the polar edge of the main ionospheric trough on the passing signals. The mechanisms (modes) of propagation are also changed during the substorm.

3. Radio propagation modeling within the substorm period was carried out using the assumption that there was a change of ionospheric ionization in the E- and F2-layers in according to so called "the main effect in the ionosphere during substorm". Calculations of the field-aligned HF scatter took into consideration the F2 region parameters of the scatterers using a modified model of the ionosphere. Results of these calculations agreed with the experimental observations.

4. The effect of signal amplitude growth up to 20–30 dB before the substorm expansion phase onset can be physically explained by both (i) a decrease of the F2-layer ionization that leads to an approach of signal frequency to the maximum observed frequency value as well as to a decrease of the signal field divergence and (ii) a growth of the F2-layer height that associated with decreasing the collision frequency. This effect could be used as a predictor of substorms for further forecasting of space weather disturbed conditions.

5. In the northern part of the Atlantic between Canada and the European part of Russia, impact of the main ionospheric trough (MIT) on the parameters of signal in the long HF radio channel under quiet conditions manifests itself in different ways. The MIT and its polar edge influence basically the azimuthal angles of radio wave arrival. On the other hand, the butt-end sunset wall of the MIT, caused by the terminator, has significant influence on the amplitude of received signals. During substorms, there are also significant amounts of irregularities that modify the propagation by altering both the polar edge and the butt-end sunset wall of the MIT.

References

Al'pert, Ya. L.: Propagation of Electromagnetic Waves and Ionosphere (in Russian), Nauka Press, Moscow, 564, 1972.

Angling, M. J., Cannon, P. S., Davies, N. C., Willink, T. J., Jodalen, V., and Lundborg, B.: Measurements of Doppler and multipath spread on oblique high-latitude HF paths and their use in characterizing data modem performance, Radio Science, 33(1), 97–107, 1998.

Anufrieva, T. A. and Shapiro B. S.: Geometrical parameters of the ionosphere F2-layer (in Russian), Nauka Press, Moscow, 91, 1976.

Blagoveshchensky, D. V.: HF radio wave propagation at the high-latitudes (in Russian), Moscow, Nauka, 192–214, 1981.

Blagoveshchensky, D. V. and Zherebtsov, G. A.: High-latitude geophysical phenomena and forecasting of HF radio channel (in Russian), Moscow, Nauka, 35–68, 1987.

Blagoveshchensky, D. V. and Borisova, T. D.: Substorm effects of ionosphere and HF propagation, Radio Science, 35(5), 1165–1171, 2000.

Blagoveshchensky, D. V., Egorova L. V., and Lukashkin V. M.: High-latitude ionospheric phenomena diagnostics by high-frequency radio wave propagation observations, Radio Sci., 27(2), 267–274, 1992.

Blagoveshchensky D. V., Borisova T. D., and Egorova, L. V.: Pre- and after substorm situations in the ionosphere and decameter radio wave propagation (in Russian), Geomagn. Aeron., 36, N4, 125–134, 1996.

Blagoveshchensky, D. V., Maltseva, O. A., and Rodger, A. S.: Ionosphere dynamics over Europe and western Asia during magnetospheric substorms 1998-1999, Ann. Geophys., 21, 1141–1151, 2003a.

Blagoveshchensky, D. V., Pirog, O. M., Polekh, N. M., and Chistyakova, L. V.: Mid-latitude effects of the May 15, 1997 magnetic storm, J. Atmos. S.-P., 65, 303–310, 2003b.

Blagoveshchensky, D. V., Vystavnoi, V. M., and Sergeeva M. A.: HF radio propagation through the auroral oval during substorms, J. Atmos. S.-P., 67, 1618–1625, 2005b.

Blagoveshchensky, D. V. and Borisova T. D.: Correction of the HF radio channel model with allowance of solar and magnetic activity (in Russian), Geomag. Aeron., 29, 696–698, 1989.

Borisova, T. D., Baranets, A. N., and Cherkashin, Yu. N.: A method of calculation of ray-tracing end energy parameters of the radio wave propagation on the long paths, in: Ionospheric Radio Wave propagation (in Russian), Nauka, Moscow, 12–20, 1986.

Buonsanto M. J.: Ionospheric storms – a review, Space Science Reviews, 88, 563–601, 1999.

Chernyshev, D. V. and Vasil'eva, T. N.: Prediction of the Maximum Critical Frequencies for W=10, 50,100,150,200 (in Russian), Nauka, Moscow, 54, 1975.

Ginzburg, V. L.: The Propagation of Electromagnetic Waves in Plasma (in Russian), Nauka Press, Moscow, 684, 1967.

Gonzalez, W. D., Joselyn, J. A., Kamide, Y., et al.: What is a geomagnetic storm?, J. Geophys. Res., 99, No. A4, 5771–5792, 1994.

Goodman, J.: HF communications–science technology, Van Nostrand Reinhold, New York, 63–78, 1992.

Halcrow, B. H. and Nisbet, J. S.: A model of F2 peak electron densities in the main trough region of the ionosphere, Radio Sci., 12, 815–821, 1977.

Hunsucker, R. D. and Hargreaves, J. K.: The high-latitude ionosphere and its effects on radio propagation. Cambridge University Press, 113–336, 2003.

Ivanov-Kholodny, G. S. and Mikhaylov, A. V.: Forecasting of the ionospheric states (in Russian), Leningrad, Gidrometeoizdat, 190, 1980.

Lastovicka, J.: Monitoring and forecasting of ionospheric space weather – effects of geomagnetic storms, J. Atmos. S.-P., 64, 667–705, 2002.

Lyons, L. R.: Substorms: Fundamental observational features, distinction from other disturbances, and external triggering, J. Geophys. Res., 101, No. A6, 13 011–13 025, 1996.

Milan, S. E., Lester, M., Jones, T. B., and Warrington, E. M.: Observation of the reduction in the available HF band on four high latitude paths during periods of geomagnetic disturbance, J. Atmos. S.-P., 60, 617–629, 1998.

Milan, S. E., Jones, T. B., Lester, M., Warrington, E. M., and Reeves, G. D.: Substorm correlated absorption on a 3200 km trans-auroral HF propagation path, Ann. Geophys. 14, 182–190,

1996.

Milan, S. E., Jones, T. B., and Warrington, E. M.: Enhanced MUF propagation of HF radio waves in the auroral zone. Journal of Atmospheric and Solar – Terrestrial Physics 59, 237–249, 1997.

Nicolet, M.: The collision frequency of electron in the ionosphere, J. Atmos. Terrest. Phys., 3, 200–211, 1953.

Rawer, K., Ramakrishnan, S., and Bilitza, D.: International Reference Ionosphere. Brussel, URSI, Cospar, 78, 1976.

Rishbeth, H. and Garriott, O. K.: Introduction to Ionospheric Physics, Academic Press New York and London, 51–146, 1969.

Siddle, D. R., Stocker, A. J., and Warrington, E. M.: The time-of-flight and direction of arrival of HF radio signals received over a path along the mid-latitude trough: observations, Radio Sci.e, 39, RS4008, doi:10.1029/2004RS003049, 2004a.

Siddle, D. R., Zaalov, N. Y., Stocker, A. J., and Warrington, E. M.: The time-of-flight and direction of arrival of HF radio signals received over a path along the mid-latitude trough: theoretical considerations, Radio Sci., 39, RS4008, doi:10.1029/2004RS003052, 2004b.

Warrington, E. M. and Stocker, A. J.: Measurements of the Doppler and multipath spread of HF signals received over a path oriented along the mid-latitude trough, Radio Sci., 38, (5), 1080, doi:10.1029/2002RS002815, 2003.